



# Towards Robust Demographic Models: A Systematic Framework to $^{14}\text{C}$ Data Aggregation and Analysis with Lessons from the Southern Levant

DATA PAPER

MAGDALENA MARIA ELISABETH BUNBURY 



**CORRESPONDING AUTHOR:**

**Dr. Magdalena Maria Elisabeth Bunbury**

Institute of Prehistoric and Protohistoric Archaeology, Kiel University, Kiel, DE; Cluster of Excellence, ROOTS – Social, Environmental, and Cultural Connectivity in Past Societies, Kiel University, Kiel, DE; Australian Research Council (ARC) Centre of Excellence for Australian Biodiversity and Heritage, James Cook University, Cairns, Queensland, AU; Australian Research Council (ARC) Centre of Excellence for Indigenous and Environmental Histories and Futures, James Cook University, Cairns, Queensland, AU

[magdalena.bunbury@jcu.edu.au](mailto:magdalena.bunbury@jcu.edu.au)

## ABSTRACT

This study presents a comprehensive seven-step framework for curating and analysing large radiocarbon ( $^{14}\text{C}$ ) datasets, optimised for generating robust *Summed Probability Distribution* (SPD) models to investigate ancient population trends and human-environment interactions. The framework is applied to a dataset of 4,657  $^{14}\text{C}$  dates from 582 archaeological sites in the Southern Levant, spanning the last 50,000 years. Key steps include  $^{14}\text{C}$  dataset fusion, duplicate elimination, dataset enhancement,  $^{14}\text{C}$  date categorisation, outlier analysis, limitation assessment, and SPD modelling and publication. These systematic processing steps ensure the dataset is transparent, standardised, and adheres to FAIR principles for accessibility and reusability. By providing a replicable methodology, the framework enhances consistency and reliability in archaeological data curation and analysis, making it adaptable to other large-scale datasets.

**KEYWORDS:**

Radiocarbon dating; Summed Probability Distribution; Phytogeographic zones; Dataset fusion; Archaeological chronologies; Population dynamics; Climate change

**TO CITE THIS ARTICLE:**

Bunbury MME 2025 Towards Robust Demographic Models: A Systematic Framework to  $^{14}\text{C}$  Data Aggregation and Analysis with Lessons from the Southern Levant. *Journal of Open Archaeology Data*, 13: 3, pp. 1–11. DOI: <https://doi.org/10.5334/joad.144>

## (1) OVERVIEW

### CONTEXT

*Summed Probability Distributions* (SPDs) generated from large radiocarbon ( $^{14}\text{C}$ ) datasets have become a critical tool for reconstructing ancient demographic trends, offering valuable insights into population dynamics, material culture distribution, settlement patterns, and palaeoclimate fluctuations [1–4]. However, the rapid expansion of  $^{14}\text{C}$  datasets—often scattered across various digital repositories—poses significant challenges for data aggregation, standardisation, and quality control [5, 6]. Moreover, many  $^{14}\text{C}$  dates lack essential contextual information, such as archaeological periodisation and environmental attributes, which limits the analytical scope and interpretive reliability of SPD-based studies.

To address these limitations, this study introduces a comprehensive seven-step framework for systematically aggregating, refining, and enhancing large  $^{14}\text{C}$  datasets. Applied to the Southern Levant, this framework compiles a dataset of 4,657  $^{14}\text{C}$  dates from 582 archaeological sites spanning the Palaeolithic to the Late Iron Age. By incorporating detailed archaeological and environmental data, the framework enables nuanced modelling of demographic trends. Two specific case studies demonstrate its utility:

- Population dynamics across mesic, semi-arid, and arid zones from approximately 11,750–3,100 cal BP (9800–1150 BCE), spanning the Neolithic to Late Bronze Age.
- Demographic trends within the Negev desert during the same period.

This structured approach tackles key challenges in  $^{14}\text{C}$  modelling—such as dataset fragmentation, outlier identification, and context-specific reliability—enhancing the accuracy of SPD models in archaeological research. The dataset, along with associated Excel and R codes, is openly accessible on [GitHub](#) and [Zenodo](#), adhering to FAIR data principles to support reproducibility and facilitate scholarly collaboration.

### Spatial coverage

[Figure 1](#) shows the distribution of 561 georeferenced archaeological sites across the Southern Levant, covering southern Syria, Lebanon, Jordan, the West Bank, and Israel. The geographic coordinate system used is WGS1984. The latitude and longitude coordinates are:

- **Northern boundary:** approximately +34.6° N, encompassing southern Syria and southern/middle Lebanon.
- **Southern boundary:** around +28.6° N, reaching southern Jordan and the southern Sinai Peninsula.

- **Eastern boundary:** around +37.1° E, covering eastern Jordan.
- **Western boundary:** approximately + 33.6° E, aligning with the Mediterranean coastline of Israel and extending westward into the Sinai Peninsula.

### Temporal coverage

The dataset spans the past 50,000 years, from the Palaeolithic to the Late Iron Age. Radiocarbon dates are calibrated to a baseline of AD 1950 (BP).

## (2) METHODS

The Southern Levant dataset was constructed by reviewing, integrating, and refining existing compilations from open-access digital repositories specific to the region. A seven-step methodological framework was developed to enhance the accuracy, transparency, and interpretative depth of  $^{14}\text{C}$  records, refining previous approaches to outlier analysis in SPD modelling [2, 7].

### STEPS

This study established a seven-step methodological framework for  $^{14}\text{C}$  dataset generation and assessment, as shown in [Figure 2](#):

1. Radiocarbon dataset fusion
2. Duplicate elimination
3. Dataset enhancement
4. Radiocarbon date categorization
5. Outlier analysis
6. Limitation analysis
7. SPD modelling and publication.

### SAMPLING STRATEGY

The sampling approach followed steps 1 through 3 of the seven-step framework ([Figure 2](#)).

#### 1. Radiocarbon dataset fusion

This project began by compiling  $^{14}\text{C}$  dates ('SouthernLevant14C') from multiple published and open-access repositories (2019 to 2022), including Radon B [8], PPND [9], CalPal (now unavailable), ORAU [10], D-REAMS [11], Flohr et al. [12], and Regev et al. [13]. Additional datasets were integrated from journal articles and the grey literature to supplement underrepresented periods, particularly from the Palaeolithic and Late Iron Age. These include studies by Boaretto et al. [14], Carmi [15], Weinstein [16], and Segal & Carmi [17, 18].

The dataset was further enriched with two major repositories published in 2022: NERD [5] and p3k  $^{14}\text{C}$  [6]. While these repositories provided valuable data, additional quality control was conducted to ensure

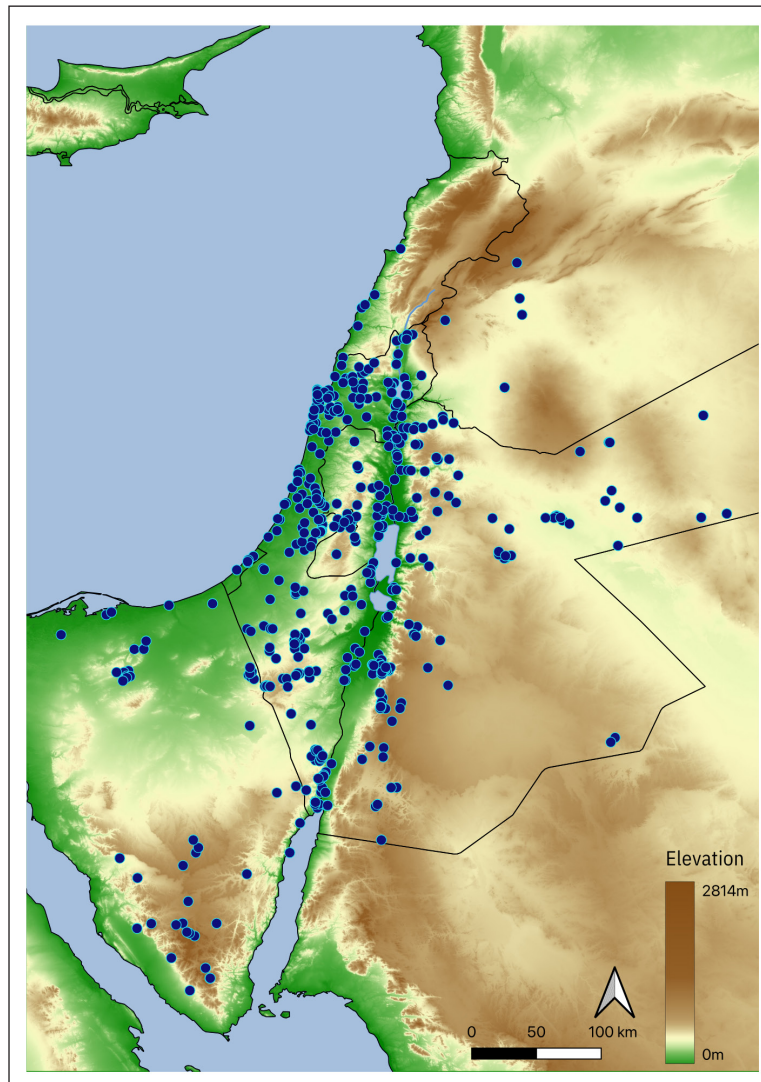


**Figure 1** The spatial distribution of 561 georeferenced radiocarbon ( $^{14}\text{C}$ )-dated archaeological sites across the Southern Levant covering southern Syria, Lebanon, Jordan, the West Bank, and Israel. The dataset spans the last 50,000 years, covering the Palaeolithic to the Late Iron Age.

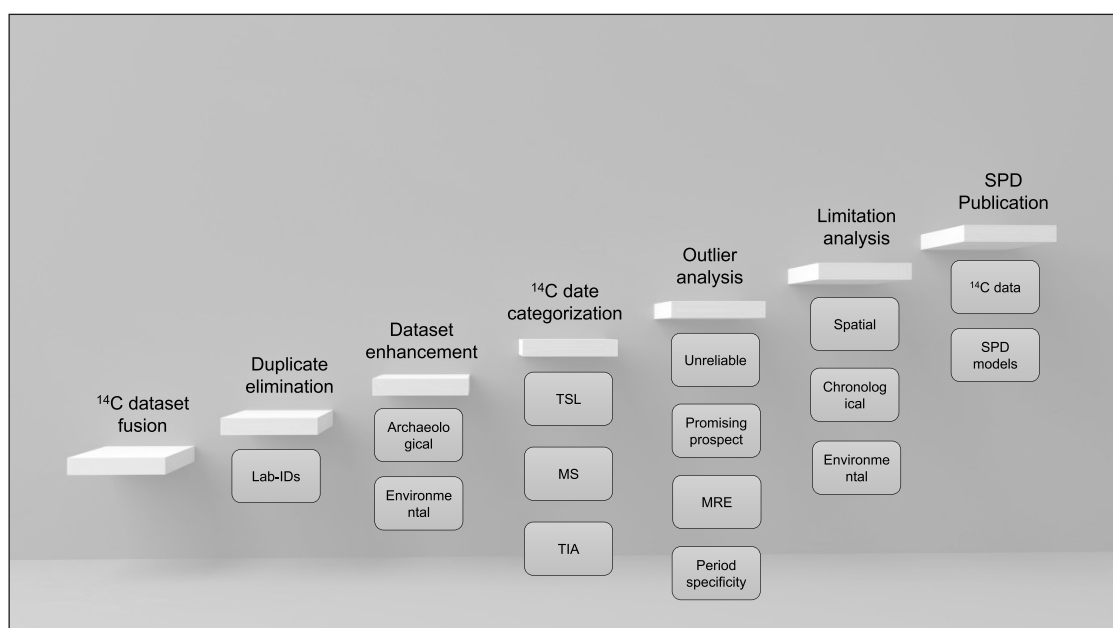


**Figure 2** Seven-step methodological framework for  $^{14}\text{C}$  dataset generation and assessment. Key abbreviations include: Marine Reservoir Effect (MRE), Marine Samples (MS), Terrestrial Samples with Inbuilt Age (TIA), and Terrestrial Short-Lived materials (TSL).

consistency. For example, NERD excludes samples with ambiguous coordinates, necessitating a comprehensive outlier analysis (step 5). Each entry was manually assessed and tagged with its source to ensure accurate chronological and geographical referencing.

## 2. Duplicate elimination

Duplicates were identified and removed by comparing laboratory IDs, Conventional Radiocarbon Age (CRA), and error values. The reconciliation of duplicates was performed using Excel, OxCal [19], and Rcarbon [20]. For samples sharing the same lab ID but with different CRA and error values, a labelling system was implemented (e.g., P-2054 (A), P-2054 (B)). Site names recorded under alternative designations (e.g., Ghassul vs. Teleilat el Ghassul) were standardised using cross-referenced CRA values, BP ranges, and contextual descriptions.

## 3. Dataset enhancement

### Geographic position

Each site was assigned a unique identifier ('Site\_ID'), and coordinates were primarily sourced from NERD [5] and p3k <sup>14</sup>C [6]. The NERD database cross-checked all spatial coordinates using existing online digital archives and publications. For Palaeolithic sites not covered by these repositories, coordinates were derived from published journal sources or manually georeferenced using Google Earth (WGS84 decimal degrees). Manual georeferencing ensured consistency with existing site descriptions, though precision may vary depending on site reporting quality.

### Phytogeographic zones

Sites were classified into phytogeographic zones (e.g. 'Mediterranean', 'Irano-Turanian', 'Saharo-Arabian', and 'Sudanean') to reflect vegetation influenced by climate (Table 1). Transitional zones [21] were cross-verified with

journal references to select the most likely classification. Additionally, moisture and humidity categories (e.g. 'Mesic', 'Semi-arid', and 'Arid') and natural geographic areas (e.g. 'Galilee', 'Jordan Valley', 'Negev') were assigned to capture local environmental variability ('Temperature\_Humidity' and 'Subregion').

### Archaeological data

Each <sup>14</sup>C sample was assigned to an archaeological period (e.g., 'Pottery Neolithic') and culture (e.g., 'Yarmukian'), captured in 'Archaeological\_Period' and 'Culture' fields. Additional information included the sample's specific archaeological context ('Archaeological\_Context'), organic material type ('Material'), calibrated radiocarbon age ('CRA'), 1-sigma error margin ('Error'), and environmental isotope variations ('δ<sup>13</sup>C' values). Intrusive <sup>14</sup>C dates were further verified to confirm accuracy. Additional fields, including 'Site\_Function' and 'Comments' on artefact types, were incorporated to provide greater functional context. However, this aspect of the dataset is still being refined.

## QUALITY CONTROL

Data integrity was ensured through steps 4 and 5 of the framework (Figure 2).

## 4. Radiocarbon date categorisation

Building on prior research [2, 7], <sup>14</sup>C samples were classified into three primary classes, allowing structured SPD generation and targeted analyses of different material types (Figure 3):

- **Class 1:** Short-lived terrestrial samples (TSL: n = 1,339)
- **Class 2:** Bone and shell samples with potential Marine or Freshwater Reservoir Effects (MRE/FRE) (MS: n = 142)

PHYTOGEOGRAPHIC ZONE	VEGETATION	NATURAL GEOGRAPHIC AREAS ('SUBREGION')	ARIDITY	PRECIPITATION	NUMBER OF <sup>14</sup> C DATES
<b>Mediterranean</b>	Mediterranean forest, maquis, and coastal scrub	Coastal plains (northern Israel, southern Lebanon, Carmel Ridge, Galilee, Samaria and Judea)	Mesic	>300 mm/year, typically 400–800 mm	728
<b>Irano-Turanian</b>	Transition zone between Mediterranean and desert ecosystems: Steppe and shrublands, including xerophytic species	Inland areas (Judean Desert, eastern Samaria, central Jordan Valley, Sea of Galilee surroundings)	Semi-arid	150–300 mm/year	1525
<b>Saharo-Arabian</b>	Sparse desert vegetation, dominated by drought-resistant species	Negev Desert, Arava Valley, parts of the Eastern desert, Sinai Peninsula	Arid	<150 mm/year (with significant areas receiving <100 mm/year)	1390
<b>Sudanian</b>	Sparse desert vegetation with occasional tropical elements	Southern Jordan Valley, Arava Valley, Rift Valley, parts of eastern Jordan	Arid	<100 mm/year (almost no rainfall)	38

Table 1 Phytogeographic zones and natural geographic areas [21, 22].

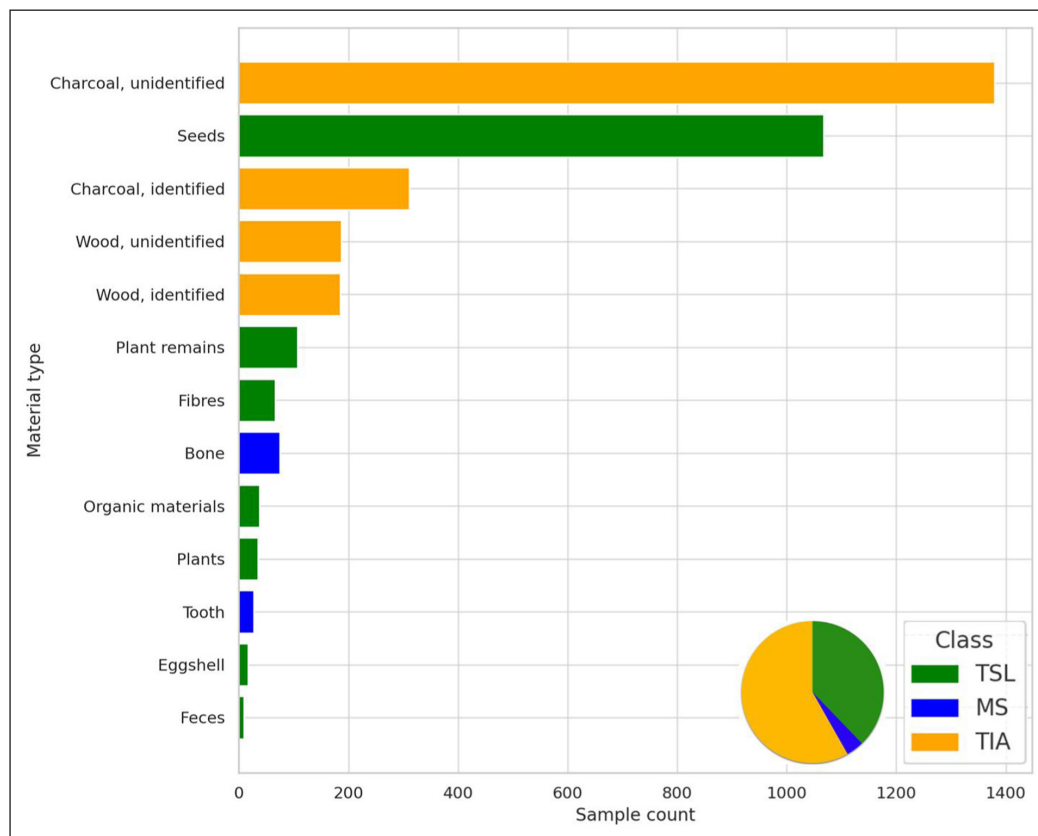


**Figure 3** Distribution of Archaeological Materials. Green bars: Terrestrial Short-Lived (TSL) samples; blue bars: (potentially) Marine Samples (MS); and orange bars: Terrestrial samples with Inbuilt Age (TIA).

- **Class 3:** Terrestrial samples with inbuilt age (TIA: n = 2,062)

Each class is subdivided into:

- **'a':** High reliability (e.g., short-lived organics with minimal inbuilt age).
- **'b':** Lower reliability (e.g., samples with greater potential for dating offsets).

## 5. Outlier analysis

Expanding on previous research [7, 23], samples were classified into four 'outlier' groups based on methodological and contextual reliability (Table 2). Here, outlier refers to  $^{14}\text{C}$  dates that exhibit reliability concerns due to dating offsets, reservoir effects, or missing contextual data, rather than statistical anomalies alone.

- **Outlier 1:** Unreliable  $^{14}\text{C}$  dates (n = 467)
- **Outlier 2:** Samples with potential reliability issues (n = 566)
- **Outlier 3:** Bone samples affected by reservoir effects (n = 65)
- **Outlier 4:** Reliable  $^{14}\text{C}$  dates lacking specific archaeological contexts.

Approximately 25% of the dataset was flagged as unreliable (n = 1,098). Additionally, Outlier 4 was excluded due to its contextual irrelevance, with clear reasons documented in the 'Outlier\_Reason' field.

## CONSTRAINTS

### 6. Limitation analysis

Chronological biases were addressed in step 6 of the framework (Figure 2) using aoristic weighting for  $^{14}\text{C}$  dates and site distributions, independent of R-based software [2, 24]. This study focuses on the period from 11,750–3,100 cal BP (9800–1150 BCE), emphasising prehistoric phases while minimising biases from Palaeolithic and Iron Age  $^{14}\text{C}$  dating. To mitigate edge effects, dates overlapping with the Neolithic or Late Bronze Age were included, even if categorised as Late Epipaleolithic or Iron Age. These dates have P values <1 due to their calibrated ranges overlapping with other periods.

### AORISTIC WEIGHTS OF $^{14}\text{C}$ DATES

The file 'AoristicWeights $^{14}\text{C}$ ' provides calibrated  $^{14}\text{C}$  dates in both cal BP and BCE at 68% and 95% probabilities. Terrestrial  $^{14}\text{C}$  dates were calibrated using the IntCal20 calibration curve [25]. To standardise the analysis, the dataset divides the timeline into 173 intervals of 50 years. Probabilities of occupation were calculated based

OUTLIER	CATEGORY	NUMBER OF <sup>14</sup> C DATES
1	Unreliable <sup>14</sup> C dates	467
1a	Questionable archaeological contexts	6
1b	Intrusive materials	96
1c	Error values, where the CRA exceeds 10%	91
1d	Mixed <sup>14</sup> C reservoirs	121
1e	Potential contamination, e.g., burnt material	153
2	Promising prospect	566
2a	Unspecified Lab-ID, CRA or error values, or potential duplicates	142
2b	Unknown site or site that is not georeferenced	91
2c	Unspecified material	327
2d	The <sup>14</sup> C date appears in databases, however there is no associated reference with it	6
3	Bone samples and reservoir effects	65
3a	Marine or freshwater species (snails, molluscs, shell)	20
3b	Burnt bone (without collagen), carbonate (inorganic carbon)	6
3c	Unspecified ΔR values of unspecified bone samples or human bone from coastal areas	33
3d	ΔR value does not point to TSL/TIA material	6
4	<sup>14</sup> C dates that do not fall into a specific archaeological period/context (e.g., 9800–1150 BCE as illustrated in <a href="#">Figures 4–5</a> )	Dependent on the research question

**Table 2** Outlier Analysis of <sup>14</sup>C dates and associated archaeological contexts.

on the earliest and latest <sup>14</sup>C dates for each site ('Earliest' and 'Latest' columns):

```
=IF(AND(N$1>=$L3, N$1<=$K3), 1/(((K3-$L3)/50)+1), 0) // Distributes probability across all 50-year intervals within the calibrated range.
```

Explanation:

- Column K: Earliest calibrated age range.
- Column L: Latest calibrated age range.
- Row 1: Defined time intervals (50-year bins).
- Columns N-GE: Probability calculations for each interval.

This formula determines the number of 50-year intervals within a site's age range ( $(K3-L3)/50$ ) and assigns probabilities by dividing 1 by the total number of intervals plus one. Only intervals within the calibrated age range receive a non-zero probability. Summing all intervals ( $=SUM(N3:N2652)$ ) provides the total occupation probability for each site across its range.

### AORISTIC WEIGHTS OF ARCHAEOLOGICAL SITES

The file 'SouthernLevantSites.csv' captures archaeological site details, including their earliest and latest occupation phases based on <sup>14</sup>C data ('Earliest' and 'Latest'). Typological data ('Chronology', 'Earliest\_Period', 'Latest\_

Period') is cross-referenced with <sup>14</sup>C data to enhance interpretation and identify occupation gaps ('Hiatus\_Occupation'). The timeline for each site is segmented into discrete phases ('Number\_Intervals\_Site'), while occupation probabilities ('Probability\_Occupied\_Intervals') refine settlement pattern analysis.

For sites with multiple <sup>14</sup>C dates, probabilities of occupation per interval were summed. For sites with hiatuses in occupation, probabilities were manually adjusted. The number of occupied intervals per site was calculated in Excel using:

```
=COUNTIF(M3:GD3,">0") // Counts the number of occupied 50-year intervals per site.
```

The standardisation of probabilities per interval was computed as:

```
=1/J3 // Normalises the probability per interval based on total intervals.
```

These calculations ensure that site occupation probabilities are standardised across varying site durations, allowing for unbiased comparison in SPD modelling.

### RATIO OF <sup>14</sup>C DATES PER SITE

The file 'Ratio14CSites.scv' quantifies the representation of time slices by combining summed probabilities from

'AoristicWeights14C.csv' and 'SouthernLevantSites.csv' (Figure 4).

Probabilities were standardised using:

```
= AVERAGE(B3:FR3) // Calculates the mean
probability across all intervals.
= STDEV.P(B3:FR3) // Computes the standard
deviation of probabilities.
```

Standardisation formula:

```
= (B3-B7) / B8 // Standardises each value by
subtracting the mean (B7) and dividing by the
standard deviation (B8).
```

Negative deviations (<-1) indicate underrepresentation, possibly due to reduced archaeological visibility or climatic events [12, 26–30]. Positive deviations (>1) suggest increased human activity (e.g. urbanisation) or improved preservation conditions [31, 32].

## 7. SPD Modelling and Publication

The SPD models derived from the Southern Levant 14C dataset provide high-resolution reconstructions of population dynamics, aligning with approaches used in previous studies [5]. By segmenting the dataset into phytogeographic zones, the SPDs reveal contrasting trends across diverse ecological regions, such as the Mediterranean, Irano-Turanian, and Saharo-Arabian zones, as well as the arid Negev desert (Figure 5B-C).

While the dataset provides robust coverage of the Southern Levant, regions like the Sudanian zone were excluded due to insufficient data ( $n = 38$ ), underscoring the challenges of studying underrepresented regions

[2, 33]. Future efforts should focus on expanding  $^{14}\text{C}$  data from these areas to enable more comprehensive comparisons.

## (3) DATASET DESCRIPTION

### OBJECT NAME

The dataset adheres to FAIR principles (Findable, Accessible, Interoperable, and Reusable) to promote transparency and reproducibility [34]. It is available on [GitHub](#) and [Zenodo](#). Zenodo ensures a Digital Object Identifier (DOI) for citation and long-term access, while GitHub allows updates for new  $^{14}\text{C}$  data or refined site information.

The dataset comprises seven files:

- **SouthernLevant14C.csv:** 4,657  $^{14}\text{C}$  dates from 582 archaeological sites.
- **AoristicWeights14C.csv:** Probability distributions for each 50-year interval.
- **AoristicWeightsSites.csv:** Probability distributions for site occupations.
- **Ratio14CSites.csv:** Standardised probabilities with statistical metrics.
- **SouthernLevantReferences.csv:** References list for  $^{14}\text{C}$  dates and sites.
- **SouthernLevantRcode:** R script for SPD generation and visualisation.
- **README.md:** Overview of the dataset structure and instructions.

### DATA TYPE

Secondary data.

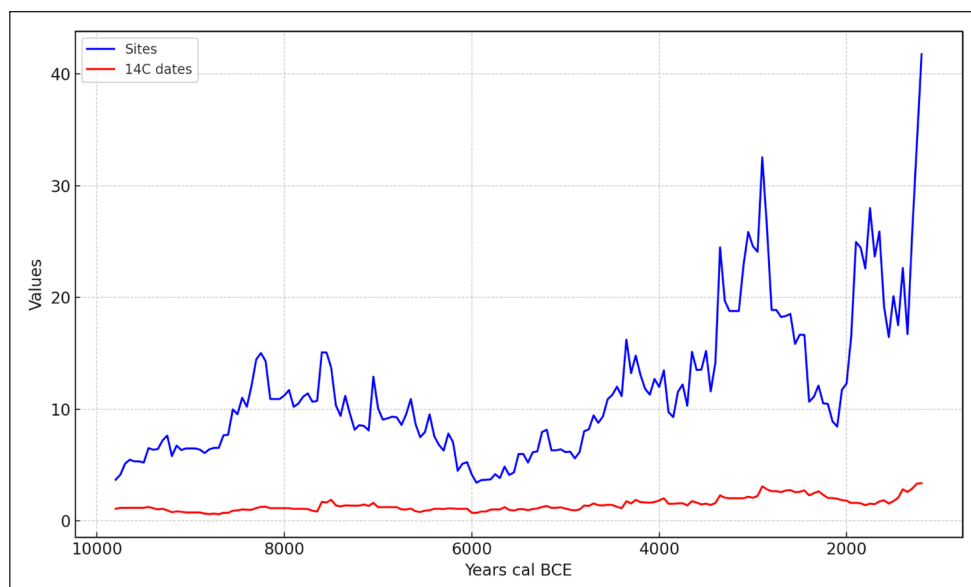


**Figure 4** Aoristic weights of  $^{14}\text{C}$ -dated sites and associated  $^{14}\text{C}$  dates. Negative deviations were recorded at 11,750–11,650 cal BP (9800–9700 BCE), 8,100–8,050 cal BP (6150–6100 BCE), and 7,950–7,450 cal BP (6000–5500 BCE). Positive deviations were observed at 5,300–4,500 cal BP (3350–2550 BCE), 3,850–3,500 cal BP (1900–1550 BCE), 3,450–3,400 cal BP (1500–1450 BCE), 3,350–3,300 cal BP (1400–1350 BCE), and 3,250–3,100 cal BP (1300–1150 BCE).

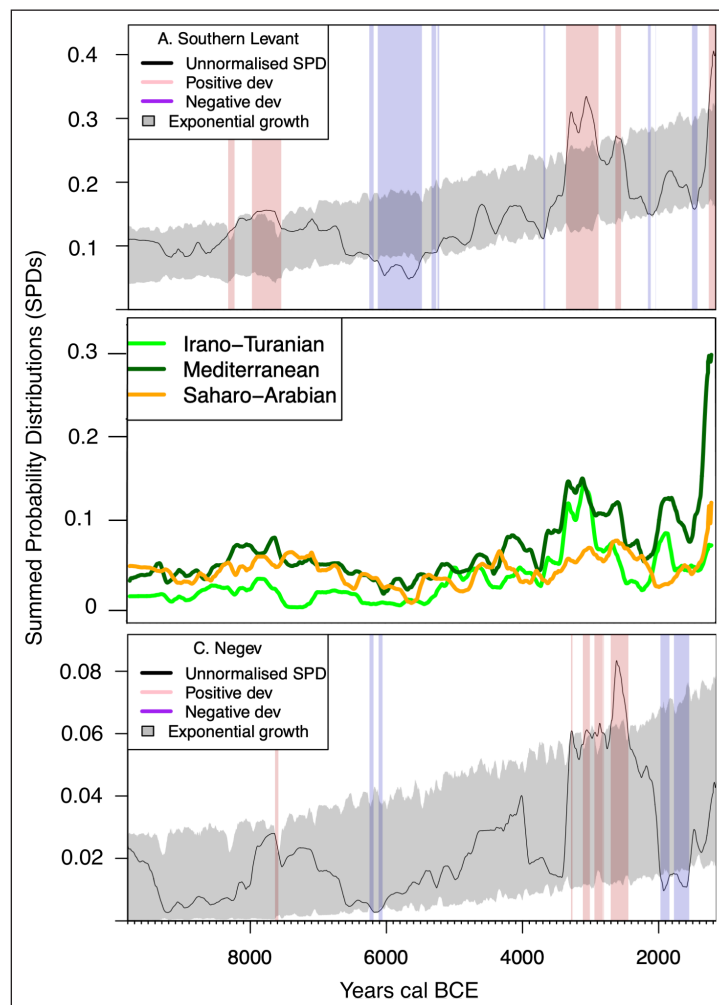


**Figure 5** Comparison of *Summed Probability Distributions (SPDs)*, 11,750–3100 cal BP (9800–1150 BCE). **A, C.** Smoothed and unnormalised SPDs, exponential fit.

A. 3,538 reliable  $^{14}\text{C}$  dates from the Southern Levant (Global p-value: 0.001).

B. Comparison of SPDs highlighting contrasting population trends across the Mediterranean ( $n = 1,724$ ), Irano-Turanian ( $n = 806$ ), and Saharo-Arabian zones ( $n = 1007$ ). The Sudanese zone is excluded due to insufficient data ( $n = 38$ ).

C. 420 reliable  $^{14}\text{C}$  dates from the Negev region (Global p-value: 0.04296).

## FORMAT NAMES AND VERSIONS

SouthernLevant14C.csv  
 AoristicWeights14C.csv  
 AoristicWeightsSites.csv  
 Ratio14CSites.csv  
 SouthernLevantReferences.csv  
 SouthernLevantRcode.R  
 README.md

## CREATION DATES

I initially compiled the Southern Levant dataset as a postdoctoral researcher at Kiel University, Germany (August 2019–March 2022). Later, while at James Cook University, Australia (June 2022–May 2024), I expanded the dataset by integrating data from NERD, p3k14C, and other sources.

## DATASET CREATORS

I, Magdalena M. E. Bunbury, conducted the data entry and managed the dataset. During my time at Kiel

University, I received guidance on data collection from Cheryl Makarewicz.

## LANGUAGE

English

## LICENSE

Creative Common License CC-BY 4.0: [15]

## REPOSITORY LOCATION

<https://doi.org/10.5281/zenodo.14053394>

## PUBLICATION DATE

08/11/2024

## (4) REUSE POTENTIAL

This  $^{14}\text{C}$  dataset offers extensive reuse potential, serving as a robust foundation for various archaeology



and interdisciplinary applications. Archaeologists can leverage its structured and contextualised data to explore prehistoric demography, settlement chronology, and socio-economic transformations, enriched by detailed site metadata and comprehensive outlier analysis.

Moreover, this dataset holds significant value for interdisciplinary research. By integrating  $^{14}\text{C}$  data with phytogeographic zones, it enables investigations into long-term environmental changes, human adaptation and societal development over millennia.

Designed to comply with FAIR principles, the dataset ensures reproducibility, accessibility, and long-term usability. Hosted on [GitHub](#) and [Zenodo](#), it provides a reliable, open-access resource to foster cross-disciplinary collaboration and advance research into ancient demographic and environmental trends.

## ACKNOWLEDGEMENTS

I thank Cheryl Makarewicz (Institute of Prehistoric and Protohistoric Archaeology, Kiel University) for her guidance during data collection, and Mara Weinelt (Institute of Prehistoric and Protohistoric Archaeology, Kiel University) for discussions on the data. I am also thankful to Julian Laabs (Department of History, Universität Leipzig) for providing essential files for map generation. Finally, I also appreciate the constructive feedback from an anonymous reviewer. Any remaining errors in the dataset remain my responsibility.


## FUNDING INFORMATION

Data collection was carried out while MMEB was funded by the Lehrstuhl in Zooarchaeology and Stable Isotope Biogeochemistry, Kiel University and the Cluster of Excellence “ROOTS – Social, Environmental, and Cultural Connectivity in Past Societies,” supported by the Deutsche Forschungsgemeinschaft (DFG, German Research Foundation) under Germany’s Excellence Strategy (EXC 2150-390870439). The final stages of data collection were completed with funding from the Centre of Excellence for Australian Biodiversity and Heritage (CABAH), supported by the Australian Research Council (ARC, CE170100015). Neither DFG nor ARC had any role in the study design, data collection and analysis, decision to publish, or manuscript preparation.

## COMPETING INTERESTS

The author has no competing interests to declare.

## AUTHOR AFFILIATIONS

**Dr. Magdalena Maria Elisabeth Bunbury**  [orcid.org/0000-0003-3114-3138](https://orcid.org/0000-0003-3114-3138)

Institute of Prehistoric and Protohistoric Archaeology, Kiel University, Kiel, DE; Cluster of Excellence, ROOTS – Social, Environmental, and Cultural Connectivity in Past Societies, Kiel University, Kiel, DE; Australian Research Council (ARC) Centre of Excellence for Australian Biodiversity and Heritage, James Cook University, Cairns, Queensland, AU; Australian Research Council (ARC) Centre of Excellence for Indigenous and Environmental Histories and Futures, James Cook University, Cairns, Queensland, AU

## REFERENCES

1. **Johannsen JW, Laabs J, Bunbury MME, Mortensen MF.** Subsistence and population development from the Middle Neolithic B (2800–2350 BCE) to the Late Neolithic (2350–1700 BCE) in Southern Scandinavia. *PLOS ONE*. 2024; 19: e0301938. DOI: <https://doi.org/10.1371/journal.pone.0301938>
2. **Bunbury MME, Austvoll KI, Jørgensen EK, Nielsen SV, Kneisel J, Weinelt M.** Understanding climate resilience in Scandinavia during the Neolithic and Early Bronze Age. *Quaternary Science Reviews*. 2023; 322: 108391. DOI: <https://doi.org/10.1016/j.quascirev.2023.108391>
3. **Palmisano A, Lawrence D, De Gruchy MW, Bevan A, Shennan S.** Holocene regional population dynamics and climatic trends in the Near East: A first comparison using archaeo-demographic proxies. *Quaternary Science Reviews*. 2021; 252: 106739. DOI: <https://doi.org/10.1016/j.quascirev.2020.106739>
4. **Timpson A, Colledge S, Crema E, Edinborough K, Kerig T, Manning K,** et al. Reconstructing regional population fluctuations in the European Neolithic using radiocarbon dates: a new case-study using an improved method. *Journal of Archaeological Science*. 2014; 52: 549–557. DOI: <https://doi.org/10.1016/j.jas.2014.08.011>
5. **Palmisano A, Bevan A, Lawrence D, Shennan S.** The NERD Dataset: Near East Radiocarbon Dates between 15,000 and 1,500 cal. yr. BP. 2022. DOI: <https://doi.org/10.5334/joad.90>
6. **Bird D, Miranda L, Vander Linden M, Robinson E, Bocinsky RK, Nicholson C,** et al. p3k14c, a synthetic global database of archaeological radiocarbon dates. *Scientific Data*. 2022; 9: 27. DOI: <https://doi.org/10.1038/s41597-022-01118-7>
7. **Bunbury MM, Petchey F, Bickler SH.** A new chronology for the Māori settlement of Aotearoa (NZ) and the potential role of climate change in demographic developments. *Proceedings of the National Academy of Sciences*. 2022; 119: e2207609119. DOI: <https://doi.org/10.1073/pnas.2207609119>
8. **Kneisel J, Hinz M, Rinne C.** Radon-B. Database accessible at: <https://radon-b.ufg.uni-kiel.de/>. 2013.

9. **Benz M.** PPNd–The platform for neolithic radiocarbon dates. *Ex Oriente*. 2014.
10. **ORAU.** Oxford Radiocarbon Accelerator Unit online database [Internet]. Oxford: University of Oxford. Available: <https://c14.arch.ox.ac.uk/database/db.php>.
11. **D-REAMS.** The Dangoor Research Accelerator Mass Spectrometry Laboratory, Weizmann Institute of Science. Rehovot, Israel; Available: <https://www.weizmann.ac.il/D-REAMS/scientific-publications>.
12. **Flohr P, Fleitmann D, Matthews R, Matthews W, Black S.** Evidence of resilience to past climate change in Southwest Asia: Early farming communities and the 9.2 and 8.2 ka events. *Quaternary Science Reviews*. 2016; 136: 23–39. DOI: <https://doi.org/10.1016/j.quascirev.2015.06.022>
13. **Regev J, De Miroschedji P, Greenberg R, Braun E, Greenhut Z, Boaretto E.** Chronology of the Early Bronze Age in the southern Levant: new analysis for a high chronology. *Radiocarbon*. 2012; 54: 525–566. DOI: <https://doi.org/10.1017/S003382220004724X>
14. **Boaretto E, Jull AT, Gilboa A, Sharon I.** Dating the Iron Age I/II transition in Israel: first intercomparison results. *Radiocarbon*. 2005; 47: 39–55. DOI: <https://doi.org/10.1017/S0033822200052188>
15. **Carmi I.** Rehovot radiocarbon measurements III. *Radiocarbon*. 1987; 29: 100–114. DOI: <https://doi.org/10.1017/S0033822200043599>
16. **Weinstein JM.** Radiocarbon dating in the southern Levant. *Radiocarbon*. 1984; 26: 297–366. DOI: <https://doi.org/10.1017/S0033822200006731>
17. **SEGAL D, CARM I.** Rehovot radiocarbon date list V. *Atiqot (Jerusalem 1991)*. 1996; 29: 79–106.
18. **Segal D, Carmi I.** Rehovot radiocarbon date list VI. *Israel Antiquities Authority Atiqot*. 2004; 48: 123–148.
19. **Ramsey CB.** Bayesian analysis of radiocarbon dates. *Radiocarbon*. 2009; 51: 337–360. DOI: <https://doi.org/10.1017/S0033822200033865>
20. **Crema ER, Bevan A.** Inference from large sets of radiocarbon dates: software and methods. *Radiocarbon*. 2021; 63: 23–39. DOI: <https://doi.org/10.1017/RDC.2020.95>
21. **Schiebel V, Litt T.** Holocene pollen record from Lake Kinneret (Sea of Galilee), Israel. *PANGAEA*; 2017. DOI: <https://doi.org/10.1594/PANGAEA.884740>
22. **Langgut D, Finkelstein I, Litt T, Neumann FH, Stein M.** Vegetation and Climate Changes during the Bronze and Iron Ages (~3600–600 BCE) in the Southern Levant Based on Palynological Records. *Radiocarbon*. 2015; 57: 217–235. DOI: [https://doi.org/10.2458/azu\\_rc.57.18555](https://doi.org/10.2458/azu_rc.57.18555)
23. **Schmid MM, Wood R, Newton AJ, Vésteinsson O, Dugmore AJ,** others. Enhancing radiocarbon chronologies of colonization: Chronometric hygiene revisited. *Radiocarbon*. 2019; 61: 629–647. DOI: <https://doi.org/10.1017/RDC.2018.129>
24. **Johnson I.** Aoristic analysis: seeds of a new approach to mapping archaeological distributions through time. 2004.
25. **Reimer PJ, Austin WE, Bard E, Bayliss A, Blackwell PG, Ramsey CB,** et al. The IntCal20 Northern Hemisphere radiocarbon age calibration curve (0–55 cal kBP). *Radiocarbon*. 2020; 62: 725–757. DOI: <https://doi.org/10.1017/RDC.2020.41>
26. **Weninger B, Alram-Stern E, Bauer E, Clare L, Danzeglocke U, Jöris O,** et al. Climate forcing due to the 8200 cal yr BP event observed at Early Neolithic sites in the eastern Mediterranean. *Quaternary Research*. 2006; 66: 401–420. DOI: <https://doi.org/10.1016/j.yqres.2006.06.009>
27. **Staubwasser M, Weiss H.** Holocene Climate and Cultural Evolution in Late Prehistoric–Early Historic West Asia. *Quaternary Research*. 2006; 66: 372–387. DOI: <https://doi.org/10.1016/j.yqres.2006.09.001>
28. **Kuijt I.** People and Space in Early Agricultural Villages: Exploring Daily Lives, Community Size, and Architecture in the Late Pre–Pottery Neolithic. *Journal of Anthropological Archaeology*. 2000; 19: 75–102. DOI: <https://doi.org/10.1006/JAAR.1999.0352>
29. **Gopher A, Gophna R.** Cultures of the eighth and seventh millennia BP in the southern Levant: A review for the 1990s. *Journal of World Prehistory*. 1993; 7: 297–353. DOI: <https://doi.org/10.1007/BF00974722>
30. **Kuijt I.** Pre–Pottery Neolithic A settlement variability: evidence for sociopolitical developments in the southern Levant. *Journal of Mediterranean Archaeology*. 1994; 7: 165–192. DOI: <https://doi.org/10.1558/jmea.v7i2.165>
31. **Gastra J, Greenfield T, Greenfield H.** There and back again: A zooarchaeological perspective on Early and Middle Bronze Age urbanism in the southern Levant. *PLoS ONE*. 2020; 15. DOI: <https://doi.org/10.1371/journal.pone.0227255>
32. **Genz H.** Cash Crop Production and Storage in the Early Bronze Age Southern Levant. *Journal of Mediterranean Archaeology*. 2003; 16: 59–78. DOI: <https://doi.org/10.1558/JMEA.V16I1.59>
33. **Williams AN.** The use of summed radiocarbon probability distributions in archaeology: a review of methods. *Journal of Archaeological Science*. 2012; 39: 578–589. DOI: <https://doi.org/10.1016/j.jas.2011.07.014>
34. **Wilkinson MD, Dumontier M, Aalbersberg IJ, Appleton G, Axton M, Baak A,** et al. The FAIR Guiding Principles for scientific data management and stewardship. *Scientific Data*. 2016; 3. DOI: <https://doi.org/10.1038/sdata.2016.18>

---

**TO CITE THIS ARTICLE:**

Bunbury MME 2025 Towards Robust Demographic Models: A Systematic Framework to <sup>14</sup>C Data Aggregation and Analysis with Lessons from the Southern Levant. *Journal of Open Archaeology Data*, 13: 3, pp. 11–11. DOI: <https://doi.org/10.5334/joad.144>

**Submitted:** 12 November 2024    **Accepted:** 18 February 2025    **Published:** 26 February 2025

**COPYRIGHT:**

© 2025 The Author(s). This is an open-access article distributed under the terms of the Creative Commons Attribution 4.0 International License (CC-BY 4.0), which permits unrestricted use, distribution, and reproduction in any medium, provided the original author and source are credited. See <http://creativecommons.org/licenses/by/4.0/>.

*Journal of Open Archaeology Data* is a peer-reviewed open access journal published by Ubiquity Press.

